HELICOPTER CONTROL WITH DYNAMIC INVERSION AND INFLOW RATE ESTIMATION

Giulio Avanzini, giulio.avanzini@unisalento.it, University of Salento (Italy)
Emanuele L. de Angelis, emanuele.deangelis4@unibo.it, University of Bologna (Italy)
Daniele Fattizzo, daniele.fattizzo2@unibo.it, University of Bologna (Italy)
Fabrizio Giulietti, fabrizio.giulietti@unibo.it, University of Bologna (Italy)

Abstract

The constant growth in the Unmanned Aerial Systems industrial sector, and the perspective of a future smart air mobility, pose a challenge in the development of increasingly reliable, robust, and performing control algorithms. Control systems landscape is extremely wide and offers several solutions for this challenge, nevertheless it is still necessary the exploration of new and more performing solutions. When a physic-based design approach is chosen for the control, paramount importance takes the knowledge of the vehicle state at every time step. Helicopter dynamics presents several inner state variables which are usually not measurable during the flight. Among these, the inflow ratio is one of the most important. Scope of this paper is the preliminary investigation of a velocity controller based on the inverse simulation of a minimum complexity model for a small-scale helicopter. An estimation of the mean induced inflow angle is also considered to improve the controller performance. The estimation is done by an extended Kalman filter. Different maneuvers have been simulated on a 11 d.o.f. helicopter model.

1. INTRODUCTION

Within an increasing air traffic context, and towards the increasing applications for unmanned vehicles, control systems require a more refined maneuvering and guidance capability. Particularly important is therefore the study of guidance and control systems capable of increasing aircraft reactivity and maneuverability, ensuring, in the meanwhile, stability and safety. The wide control systems landscape offers several solutions, but industry face up most of the projects using traditional control systems mostly based on PID logic. The success of these systems lies on their simplicity, robustness, and wide applicability. On the other hand, especially when a physic-based control is selected, very important is the knowledge of the vehicle state during the flight. Helicopter dynamics is highly non-linear and, with respect to conventional fixed-wing aircraft, it presents many additional state variables, such as the flapping angles and flapping angular rate, which are usually unknown onboard. Among these, the inflow angle is one of the inner variables which mostly affect helicopter behavior. The complexity of the airflow through the rotor disk, makes the prediction of the real inflow distribution a very demanding task. A good estimation, at least of the mean inflow value, could be already very useful for several applications. The work proposed here, is the preliminary study of a mean inflow angle estimation algorithm based on a minimum complexity model and its application in the development of a dynamic inversion controller.

Section 2 gives a brief presentation of the helicopter simulation model, the reduced order model for the dynamic inversion and the extended Kalman filter developed for the inflow rate estimation. Section 3 shows the main simulations results while conclusions are reported in Section 4.

2. MATHEMATICAL MODELS

2.1. Helicopter dynamics model

Helicopter dynamics model for simulations is based on [1]. The state and commands vectors for the model are given by:

(1) $$\boldsymbol{x} = [\boldsymbol{v_G}\,;\boldsymbol{\omega};\ \Omega_{mr};\boldsymbol{a};\ \lambda_i]$$

(2) $$\boldsymbol{u} = [\theta_0;\ A_{1s};\ B_{1s};\ \theta_{tr}]$$

Where $\boldsymbol{v_G} = [u\ v\ w]'$ and $\boldsymbol{\omega} = [p\ q\ r]'$ are the rigid body state variables in body axes, Ω_{mr} is the main rotor angular rate, $\boldsymbol{a} = [a_0\ a_1\ b_1]'$ is the flapping coefficients vector and λ_i is the mean induced inflow ratio of the main rotor. The command vector components are the main rotor collective, the lateral and longitudinal pitch and the tail rotor pitch.

The flapping angle of the blade at azimuth angle ψ at time t is modelled according to a tip-path-plane representation:

(3) $$\beta(t,\psi) = a_0(t) + a_1(t)\cdot cos(\psi) + b_1(\mathrm{t})\cdot \sin(\psi)$$

The dynamic equations of the system are:

(4) $$\dot{\boldsymbol{v}}_{\boldsymbol{G}} = \frac{\boldsymbol{F_{tot}} - \boldsymbol{\omega}\times\boldsymbol{v_G}}{m}$$

(5) $$\dot{\boldsymbol{\omega}} = \boldsymbol{I^{-1}}\{\boldsymbol{M_{tot}} - \boldsymbol{\omega}\times(\boldsymbol{I\omega})\}$$

(6) $$\dot{\Omega}_{mr} = \frac{Q_e - (Q_{mr} + \tau Q_{tr})}{I_{mr} + \tau^2 I_{tr}}$$

(7) $$\ddot{\boldsymbol{a}} = -\boldsymbol{D}\dot{\boldsymbol{a}} - \boldsymbol{K}\boldsymbol{a} + \boldsymbol{f}$$

with $\boldsymbol{D}, \boldsymbol{K}, \boldsymbol{f}$ flapping matices of [1].

(8) $$\dot{\lambda}_i = f_\lambda(x,\dot{x},u) = \frac{3\pi}{4}\left\{\frac{C_t}{2} - \lambda_i\sqrt{\mu^2+\lambda^2}\right\}$$

Where C_t is the main rotor thrust coefficient,

$\mu \doteq \sqrt{u_h^2 + v_h^2}$ is the main rotor advance ratio and $\lambda \doteq \frac{w_h}{\Omega R} - \lambda_i$ is the total inflow mean angle, both written in the main rotor hub reference frame. The inflow dynamics derives from [2] where only the mean inflow term with respect to the rotor disk distribution has been taken into account.

The total force and moment of the rigid body dynamics equations (4)(5) are composed by the weight force plus the main rotor, tail rotor and fuselage forces and moments calculated as in [1]. The engine torque Q_e in the rotor dynamics equation (6) usually equilibrates rotors aerodynamic torque and $\dot{\Omega}_{mr} = 0$ is taken, imposing and ideal behavior of the rotor speed controller. Only in case of engine failure such as during autorotation the engine torque is put zero and the rotational dynamics is considered.

Fuselage forces and moments are evaluated as a function of the angle of attack and the sideslip angle. Aerodynamic coefficients are derived from [3] where a small-scale helicopter fuselage is studied.

2.2. NDI controller architecture

A global scheme of the control system for the helicopter is reported in Figure 1. Here an inner loop controls the attitude of the helicopter, while an external loop is added for the velocity control. The roll and pitch controllers, as for the heading hold, are traditional PID based control logics. The velocity controller is instead based on a non-linear dynamic inversion (NDI) algorithm. The schemes of the attitude controllers are reported in Figure 2 and Figure 3 while the dynamic inversion-based velocity controller and its components are shown in Figure 4. Here the dynamic inversion permits to calculate reference roll and pitch angles, and the collective pitch to track a desired velocity trajectory. An integrator on the velocity error is also added to reduce steady-state error due to unmodeled dynamics. An extended Kalman filter is also added for the estimation of the inflow angle at every time step.

2.3. Reduced order model dynamic inversion

A reduced order model for the non-linear dynamic inversion controller is considered for the purposes of the present work. A three translational degrees of freedom model has been adopted and a minimum complexity model for the main rotor and tail rotor thrust and helicopter forces system has been selected. The state vector is here represented by the linear velocities while rotational velocities, rotor angular rate and inflow ratio are treated as measurable or estimable variables. The main rotor collective pitch and the Euler angles represent the input of the system. The dynamic equations written in the local vertical reference frame are:

(9) $$\begin{cases} \dot{v}_x = \frac{1}{m}(T_s\,cos\theta\ -\ T_c\,cos\phi sin\theta - T_{tr} sin\phi sin\theta) \\ \dot{v}_y = \frac{1}{m}(T_c sin\phi - T_{tr} cos\phi) \\ \dot{v}_z = g - \frac{1}{m}(T_s sin\theta\ +\ T_c cos\phi cos\theta + T_{tr} cos\theta sin\phi) \end{cases}$$

Where main rotor thrust components in the vertical local frame are given as:

(10) $$\begin{aligned} T_s &= T\sin i_s \\ T_c &= T\cos i_s \end{aligned}$$

provided T and i_s, the thrust and the shaft tilt angle respectively. Main rotort thrust model is modeled as follows, [4]:

$$T = \rho A \sigma (\Omega R)^2 \frac{Cl_\alpha}{4}\left\{\frac{2}{3}\theta_0 \frac{1-\mu^2+9\mu^4/4}{1+3\mu^2/2} + \lambda \frac{1-\mu^2/2}{1+3\mu^2/2}\right\} \tag{11}$$

For the tail rotor thrust, an implicit system of two equations for the thrust coefficient and the inflow ratio should be numerically solved:

$$\begin{cases} \lambda_{i,tr} = \dfrac{C_{t,tr}}{2\sqrt{\mu_{tr}^2 + \left(\frac{v_{tr}}{\Omega_{tr} R_{tr}} + \lambda_{i,tr}\right)^2}} \\ C_{t,tr} = \frac{Cl_\alpha \sigma}{4}\left\{\frac{2}{3}\theta_{tr}\left(1+\frac{3}{2}\mu^2\right) - \frac{v_{tr}}{\Omega_{tr} R_{tr}} - \lambda_{i,tr}\right\} \end{cases} \tag{12}$$

Considering the limited effect of the tail rotor force on the translational dynamics of the helicopter, a rough simplification is here made neglecting the effect of μ_{tr} and v_{tr}in the first equation (as it is for hovering). This allows to solve a quadratic problem obtaining:

$$C_{t,tr} \cong a + \frac{b^2}{4}\sqrt{1-\frac{8a}{b^2}} \tag{13}$$

$$T_{tr} = \rho A_{tr} \Omega_{tr}^2 R_{tr}^2 C_{t,tr} \tag{14}$$

where

$$a = \frac{Cl_\alpha \sigma_{tr}}{4}\left\{\frac{2}{3}\theta_{tr}\left(1+\frac{3}{2}\mu_{tr}^2\right) - \frac{v_{tr}}{\Omega_{tr} R_{tr}}\right\}$$

$$b = -\frac{Cl_\alpha \sigma_{tr}}{4}$$

The tail rotor thrust depends on its pitch command which is given by the heading hold controller at every time step. So, in this model the tail is not directly controlled.

The presented minimum complexity model can be inverted and used for the implementation of a velocity controller as shown in Figure 1. This controller receives a desired velocity and calculates the collective pitch and a reference attitude for the inner loop controller.

If a desired velocity needs to be tracked, a corresponding desired acceleration can be calculated starting from the actual velocity as:

$$\dot{\boldsymbol{v}}^{\boldsymbol{des}} = \left[\frac{v_x^{des} - v_x}{\tau_x}; \frac{v_y^{des} - v_y}{\tau_y}; \frac{v_z^{des} - v_z}{\tau_z}\right] \tag{15}$$

Where τ_x, τ_y, τ_z are time constants to choose.

For the dynamic inversion we impose $\dot{\boldsymbol{v}} = \dot{\boldsymbol{v}}^{\boldsymbol{des}}$ in equation (9) obtaining the compact form:

$$m\dot{\boldsymbol{v}}^{des} = \boldsymbol{f_{mr}} + \boldsymbol{f_{tr}} + m\boldsymbol{g} \tag{16}$$

The terms $\boldsymbol{f_{mr}}$ and $\boldsymbol{f_{tr}}$ depend on the Euler angles but, considering that $\boldsymbol{f_{tr}}$ has a less impact on the dynamics and making the hypothesis of limited rotational speeds during the maneuvers, it is possible to use the Euler angles at the previous instant to approximate the tail rotor contribution:

$$\boldsymbol{f}_{tr}(\theta_t, \phi_t) \cong \boldsymbol{f}_{tr}(\theta_{t-1}, \phi_{t-1}) \tag{17}$$

So $\boldsymbol{f}_{tr}$ depends on known (measurable) values and the main rotor thrust is calculated as:

$$T = \|\boldsymbol{f}_{mr}\| = \|m(\dot{\boldsymbol{v}}^{des} - \boldsymbol{g}) - \boldsymbol{f}_{tr}\| \tag{18}$$

Once the main rotor thrust is known, it is possible to invert equation (11) to obtain the collective pitch:

$$\theta_0 = \frac{3}{2}\left(\frac{1+3\mu^2/2}{1-\mu^2+9\mu^4/4}\right)\left\{\frac{T}{\rho A \sigma (\Omega R)^2 \frac{Cl_\alpha}{4}} - \lambda \frac{1-\mu^2/2}{1+3\mu^2/2}\right\} \tag{19}$$

Inverting the second equation of the system (16) under the hypothesis of small roll angles we have:

$$\phi \cong \frac{m\dot{v}_y^{des} + T_{tr}}{T \cos i_s} \tag{20}$$

Finally, rewriting the first equation of (16) in the body reference frame and again considering small pitch angles we have:

$$\theta \cong \frac{T \sin i_s - m\dot{v}_x^{des}}{m(g - \dot{v}_z^{des})} \tag{21}$$

Using equations (18)-(21) it is possible to calculate at every time step a reference attitude and collective pitch to track the desired velocity.

2.4. Inflow ratio estimation

Along dynamic inversion process, once the main rotor thrust has been calculated, the collective pitch needed for that thrust is given by equation (19). Here the inflow ratio $\lambda \doteq \frac{w_h}{\Omega R} - \lambda_i$ needs to be known. The induced term λ_i is usually not measurable, and an estimation should be done. For this purpose, an extended Kalman filter is adopted here. The dynamics of the inflow is given by equation (8) where C_t can be calculated from the thrust which is obtained as:

$$\hat{T} = \left\|m(\hat{\boldsymbol{v}} - \boldsymbol{g}) - \hat{\boldsymbol{f}}_{tr}\right\| \tag{22}$$

where the accelerations are measured, and the tail rotor force depends on measured attitude, velocities and the tail rotor pitch which is known.

The filter consists of two steps:

Measurement update: correction

$$\begin{gathered} K_k = P_k^- H_k^T (H_k P_k^- H_k^T + R)^{-1} \\ \hat{x}_k = \hat{x}_k^- + K_k (z_k - H_k \hat{x}_k^-) \\ P_k = (1 - K_k H_k) P_k^- \end{gathered} \tag{23}$$

Time propagation: prediction

(24)
$$\hat{x}_{k+1}^{-} = \Phi_k \hat{x}_k$$
$$P_{k+1}^{-} = \Phi_k P_k \Phi_k^T + Q$$

Where

$$\Phi_k = 1 + \left(\frac{df_{\lambda_i}}{d\lambda_i}\right)_k \Delta t$$

is the transition matrix, $H_k = 1$ is the measurement matrix, P is the error covariance matrix, and Q, and R are the process and measurement matrices respectively. The measure z_k is a fictious measure obtained inverting equation (11) for λ and then λ_i:

(25)
$$\hat{\lambda} = \left(\frac{1+3\mu^2/2}{1-\mu^2/2}\right)\left\{\frac{\hat{T}}{\rho A\sigma(\Omega R)^2\frac{Cl\alpha}{4}} - \frac{2}{3}\theta_0\left(\frac{1-\mu^2+9\mu^4/4}{1+3\mu^2/2}\right)\right\}$$

(26)
$$z = \lambda_i = \frac{w_h}{\Omega R} - \hat{\lambda}$$

where the thrust is calculated as in (22) while the collective, the vertical velocity in hub frame and the rotor speed are known/measured.

3. SIMULATIONS AND RESULTS

3.1. Introduction

Several simulations have been conducted to investigate the validity of the purposed approach for a small scale helicopter control. The helicopter is a Saab Goblin 700 and its main parameters are reported in Tables 1-3.

3.2. Response to step input

Starting from a level flight condition with an advancing velocity of 5 m/s, the system receives a step input on the velocity components of the three vertical local directions. Results are shown in Figure 5 and Figure 6. In the first one the desired and actual velocities are compared, and the same is done with the roll and pitch angle and yaw rate which should follow the references provided by the NDI controller. As visible, the controller works adequately following the reference velocity, even if with small overshoots. Figure 6 shows the commands given to the helicopter and the behavior of the extended Kalman filter for the mean induced inflow ratio estimation. Here it is visible how a good estimation of the inflow ratio (error less then 2%) is achieved after few seconds. During the first 10 seconds the error on the inflow generates an error on the vertical velocity. The filter needs these initial 10 seconds to reach a good estimation of the inflow and to avoid errors on the vertical control.

3.3. Slalom manoeuver

In Figure 7 and Figure 8 it is reported the slalom maneuver. The helicopter, initially in level flight, keeps its advancing velocity and follows a sinusoidal lateral velocity reference with a minimum steady state error, which is due to the unmodeled dynamics of the dynamic inversion algorithm. A good tracking capability is then verified for lateral maneuvers. Again, a good estimation of the induced inflow ratio is obtained as reported in Figure 8.

3.4. Autorotation manoeuver

The autorotation maneuver is based on results shown in [5]. The maneuver is divided in two main phases: the steady descent and the flare. In the first one, after the engine failure, the advancing and vertical velocities together with the rotor angular rate need to be kept constant. During the flare, which should start at a proper altitude, the velocity is reduced exploiting the stored kinetic energy of the rotor and landing with minimum velocity. The steady descent condition is here performed imposing to the NDI controller a constant target velocity while during the flare, the target velocity has the following form:

(27)
$$v_x^{des} = \alpha_x h^2 + \beta_x h + \gamma_x$$
$$v_y^{des} = 0$$
$$v_z^{des} = \alpha_z h^2 + \beta_z h + \gamma_z$$

So, it depends on the measured altitude and few parameters which can be chosen even considering continuity conditions with the steady descent velocities.

In Figure 9 and Figure 10 the main results are reported. Here it is visible how the controller correctly brings the helicopter from the steady descent condition to the flare phase performing a good landing with minimum velocity. For the inflow estimation, worse results are obtained in this manoeuvre. A not negligible residual error is kept during all the manoeuvre generating slight differences between the desired velocities and the obtained ones, even if not preventing a good touch-down. This probably depends on the not-negligible effect of the fuselage on the longitudinal dynamics. Further refinements need to be explored for this reason.

4. CONCLUSIONS

Scope of this paper was the development of a velocity controller based on the dynamic inversion of a minimum complexity helicopter model. The quality of the controller has been enhanced implementing an extended Kalman filter for the estimation of the mean inflow ratio, one of the key inner variables on the helicopter dynamics. The simulations on a 11 d.o.f.s helicopter model, for a small-scale helicopter, have shown a good performance of the controller for both longitudinal and lateral maneuvers. In the step response simulation and in the lateral slalom maneuver, the estimation of the inflow angle gave satisfying results when compared with the simulated uniform dynamic inflow. Worse results are obtained in the autorotation maneuver, where the estimated inflow follows the trend of the simulated one with a non-negligible steady state error, even if a good landing is achieved. This could be dependent on the effect of the fuselage which has been neglected in the low order model.

Further investigation needs to be done to improve the inflow rate estimation technique. Moreover, the technique should be validated even in a more complex simulation environment, where a more refined dynamic model for the inflow simulation should be considered.

The globally good results of the controller and the inflow rate estimation, demonstrates the good possibilities of the proposed approach and the necessity of further research and development.

5. ACKNOWLEDGMENTS

This study was carried out within the MOST - Sustainable Mobility National Research Center and received funding from the European Union Next-GenerationEU (PIANO NAZIONALE DI RIPRESA E RESILIENZA (PNRR) - MISSIONE 4 COMPONENTE 2, INVESTIMENTO 1.4 - D.D. 1033 17/06/2022, CN00000023). This manuscript reflects only the authors' views and opinions, neither the European Union nor the European Commission can be considered responsible for them.

6. REFERENCES

[1] P. D. Talbot, B. E. Tinling, W. A. Decker e R. T. N. Chen, «A mathematical model for a single main rotor helicopter for piloted simulation,» Ames Reasearch Center, Moffett, Field, California, September 1982.

[2] D. Peters e N. HaQuang, «Dynamic Inflow for practical applications,» *Journal of American Helicopter Society TN,* October 1988.

[3] R. Reβ, M. Grawunder e C. Breitsamter, «Aerodynamic analysis of a helicopter,» *Progress in Flight Physics,* vol. 7, pp. 99-110, 2015.

[4] A. Bramwell, G. Done and D. Balmford, Bramwell's Helicopter Dynamics, second ed., Butterworth-Heinemann, 2000, pp. 77-136.

[5] G. Avanzini, E. de Angelis, D. Fattizzo e F. Giulietti, «Autorotation design and simulation for a small-scale helicopter,» in *48th European Rotorcraft Forum*, Winthertur, Switzerland, 2022.

[6] R. T. N. Chen, «A simplified rotor system mathematical model for piloted flight dynamics simulation,» Ames Reaserach Center, NASA, Moffett Field, California, May 1979.

[7] R. T. N. Chen, «Effects of primary rotor parameters on Flapping Dynamics,» *NASA Technical Paper 1431,* January 1980.

[8] P. Simplício, M. Pavel, E. Van Kampen e Q. Chu, «An acceleration measurements-based approach for helicopter,» *Control Engineering Practice,* vol. 1, n. 8, pp. 1065-1077, 2013.

[9] D. Thomson e R. Bradley, «Inverse simulation as a tool for flight dynamics research—Principles and applications,» *Progres in Aerospace Science,* vol. 2, n. 3, 2006.

[10] G. Avanzini e G. de Matteis, «Two-Timescale Inverse Simulation of a Helicopter Model,» *Journal of guidance, control and,* vol. 24, n. 2, 2001.

[11] G. Avanzini, D. Thomson e A. Torasso, «Model Predictive Control Architecture for Rotorcraft Inverse Simulation,» *Journal,* August 2011.

[12] T. M. Giulietti F., «Coupled GPS/INS integration for Unmanned Aerial Vehicle Applications,» in *International Symposium on Light Weight Unmanned Aerial Systems and Subsystems*, 2009.

Table 1: Helicopter inertial properties

Parameters		Value	Unit
Total mass	M_{tot}	4.8	kg
Inertia moments	I_{xx}	0.0465	$kg \cdot m^2$
	I_{yy}	0.2971	$kg \cdot m^2$
	I_{zz}	0.2567	$kg \cdot m^2$
Inertia products	I_{xy}	0.0079	$kg \cdot m^2$
	I_{xz}	0.0033	$kg \cdot m^2$
	I_{yz}	-0.0006	$kg \cdot m^2$

Table 2: Tail rotor parameters

Parameters		Value	Unit
Tail Rotor speed in normal flight	$\Omega_{tr,100\%}$	736	$\frac{rad}{s}$
Tail Rotor Radius	R_{tr}	0.115	m
Number of blades	$N_{b\,tr}$	2	$--$
Tail Rotor solidity	σ_{tr}	0.1716	$--$
Tail rotor position in body axes	$r_{tr} = \begin{bmatrix} x_h \\ y_h \\ z_h \end{bmatrix}$	$\begin{bmatrix} -1.045 \\ 0.052 \\ -0.031 \end{bmatrix}$	m

Table 3: Main rotor parameters

Parameters		Value		Unit
Rotation direction	χ	$-1\ Clockwise$		$--$
Rotor speed in normal flight	$\Omega_{100\%}$	147		$\frac{rad}{s}$
Radius	R	0.79		m
Rotational Inertia	I_{mr}	0.0689		$kg \cdot m^2$
Number of blades	N_b	2		$--$
Virtual Hinge Off-set ratio	ε	0.0314		$--$
Airfoil lift slope	Cl_α	2π		$1/rad$
Airfoil chord	c	0.06		m
Blade mass	m_b	0.2057		kg
Blade in-ertia about flapping hinge	I_b	0.0344		$kg \cdot m^2$
Flapping stiffness	K_β	162.69		$N \cdot m / rad$
Pitch-Flap coupling	K_1	0		$--$
Blade twist	θ_t	0		rad/m
Rotor so-lidity	σ	0.0479		$--$
Rotor shaft tilt angle	i_s	0.0524		rad
Precone	a_0	0		rad
Hub posi-tion in body axes	$r_h = \begin{bmatrix} x_h \\ y_h \\ z_h \end{bmatrix}$	$\begin{bmatrix} 0.0095 \\ 0 \\ -0.1810 \end{bmatrix}$		m

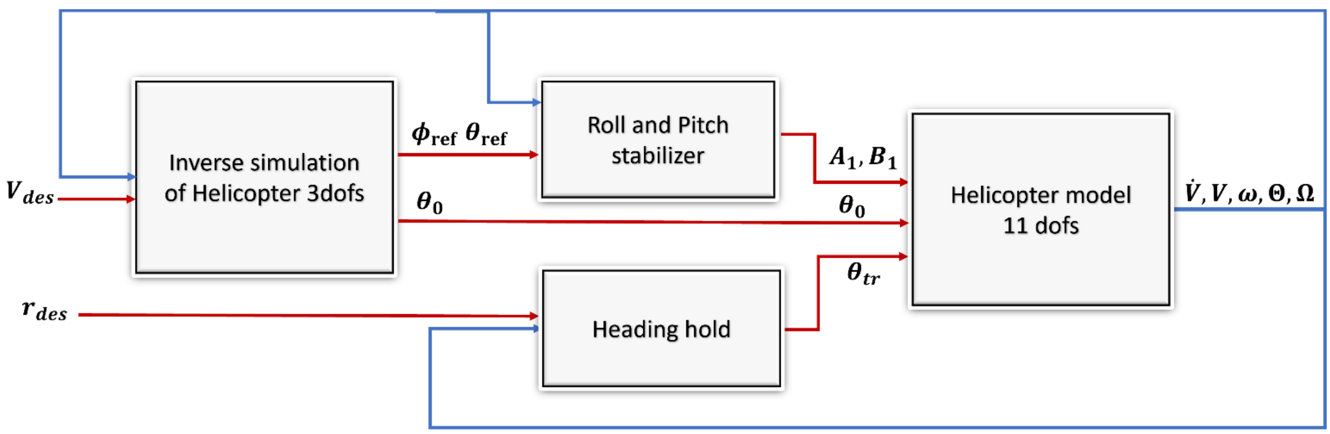

Figure 1: Global control scheme

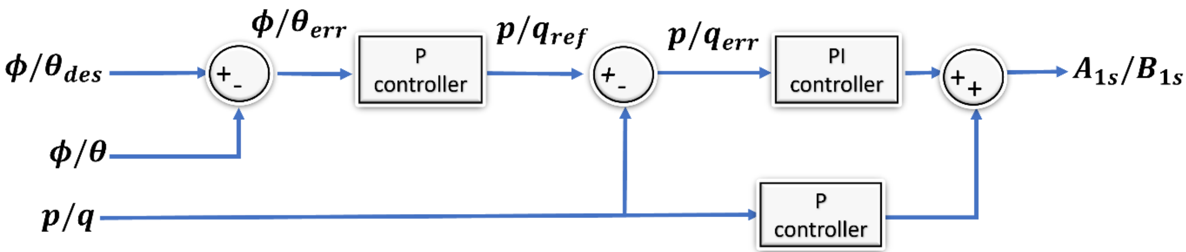

Figure 2: Pitch and roll stabilizer

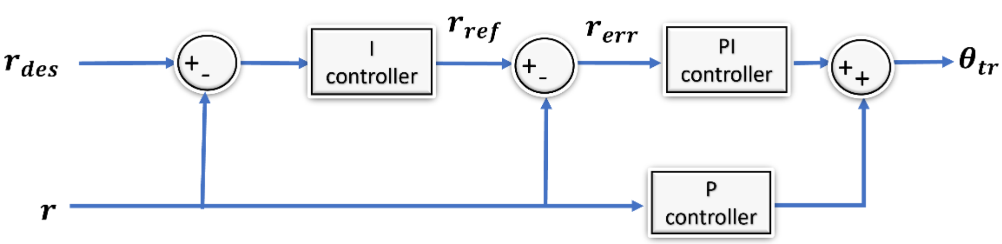

Figure 3: Heading hold controller

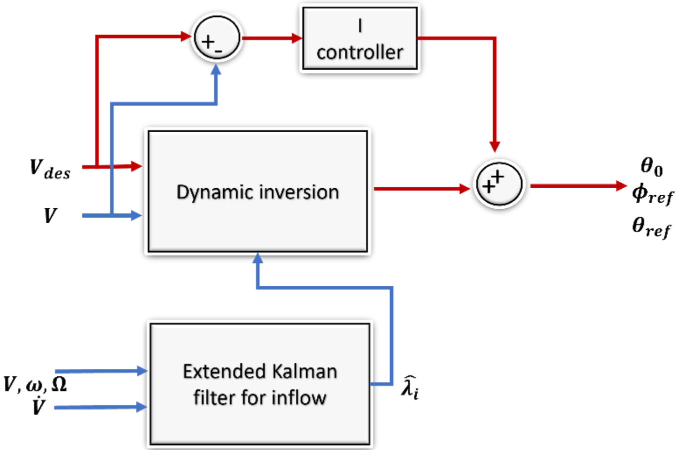

Figure 4: Velocity controller with dynamic inversion and inflow estimation

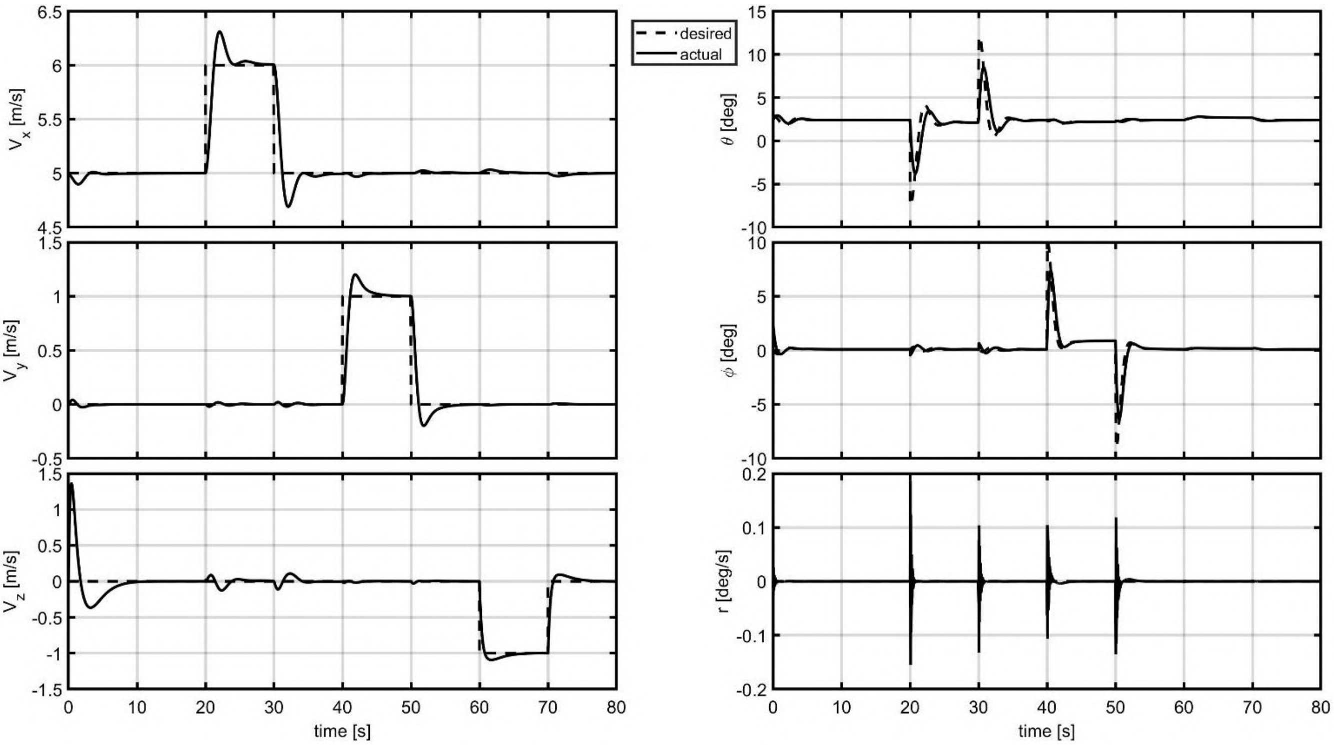

Figure 5: Velocity and Attitude response to step inputs

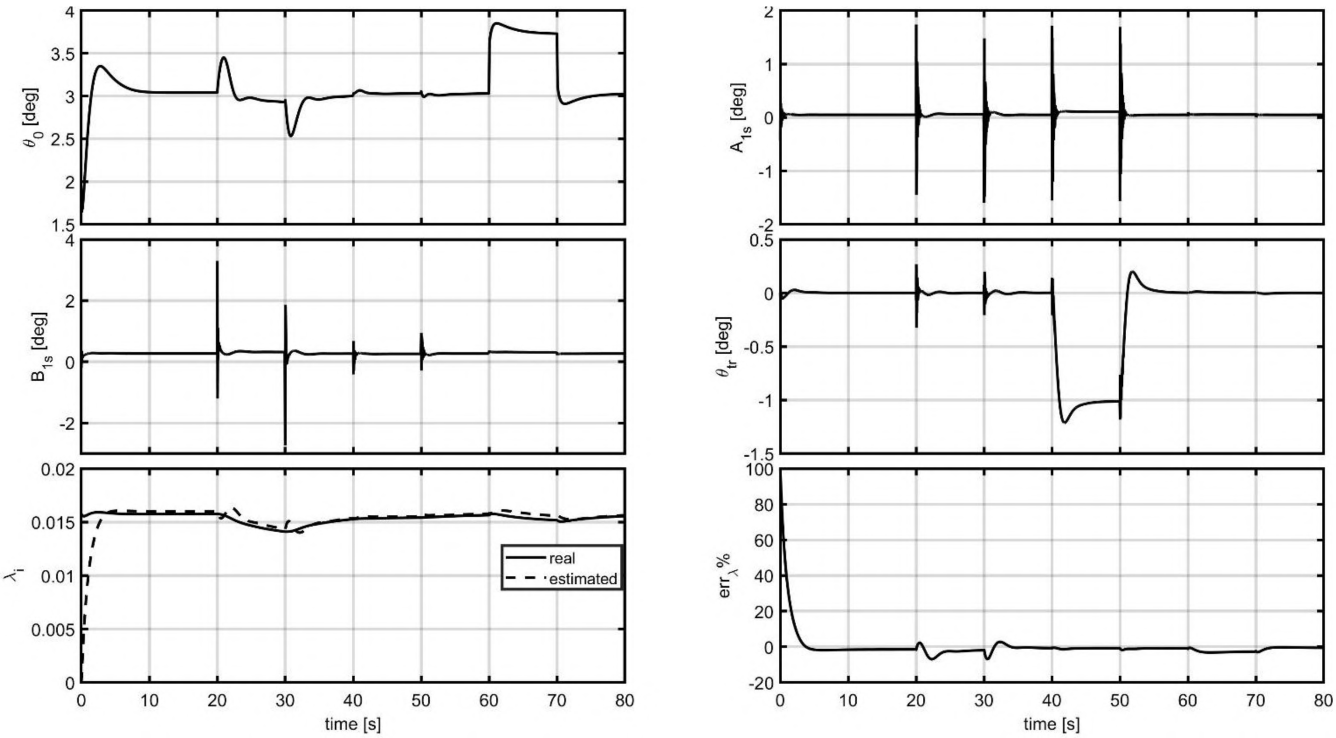

Figure 6: Commands and inflow estimation for step inputs

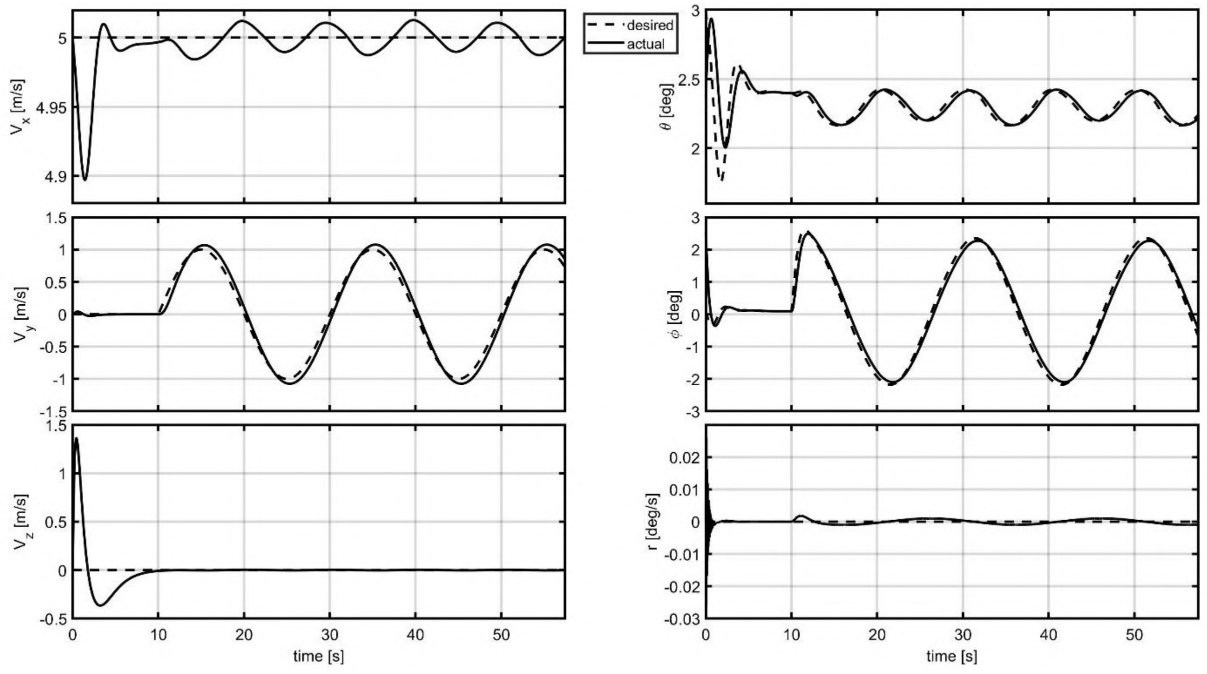

Figure 7: Velocity and attitude for a lateral slalom maneuver

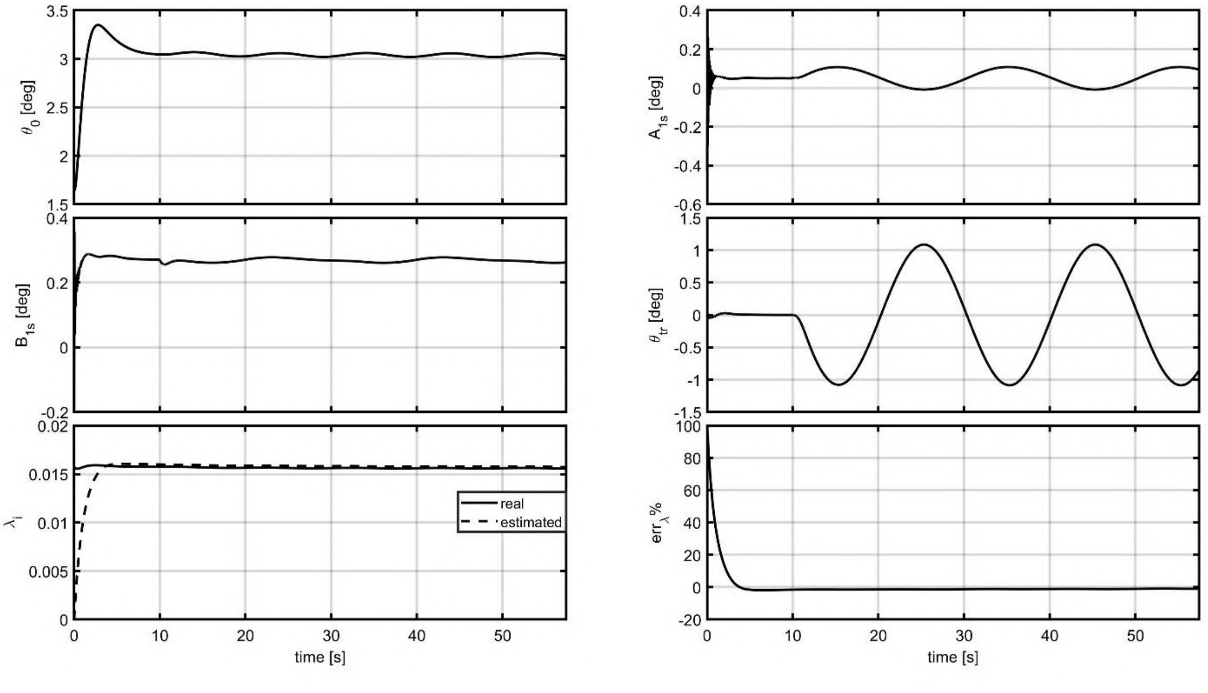

Figure 8: Commands and inflow estimation for lateral slalom maneuver

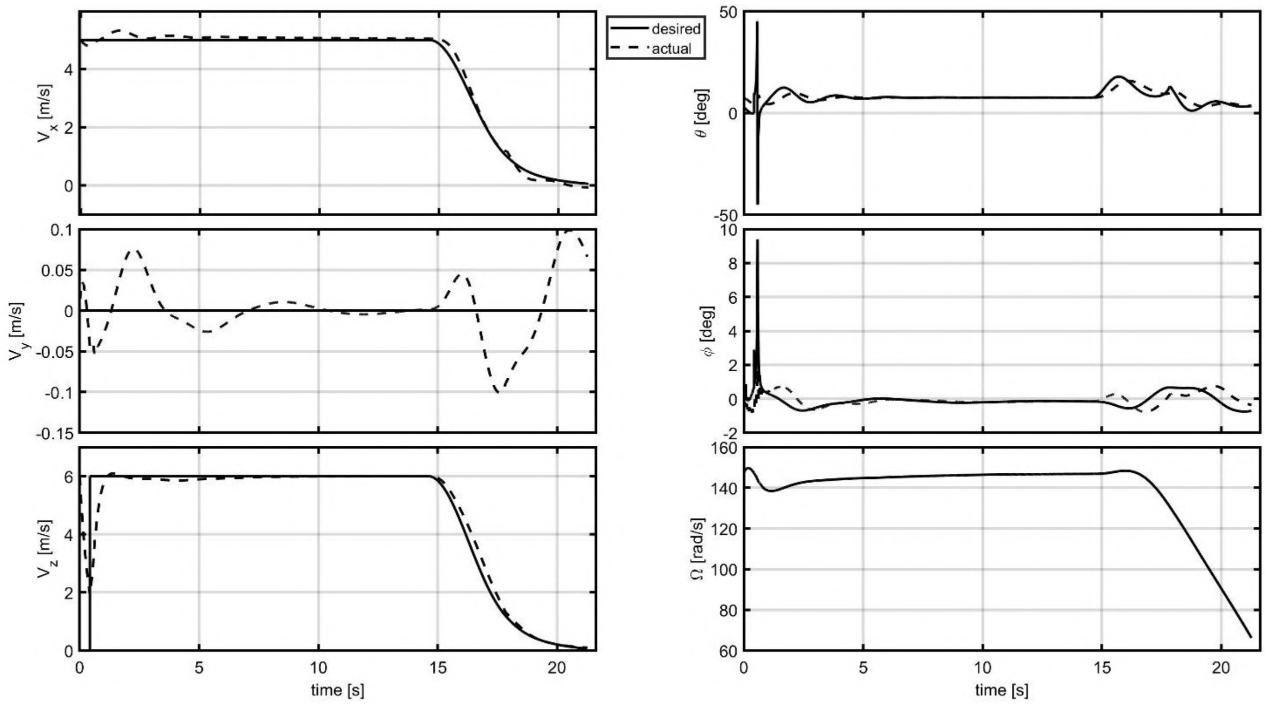

Figure 9: Velocity, atittude and rotor angular rate for the autorotation maneuver

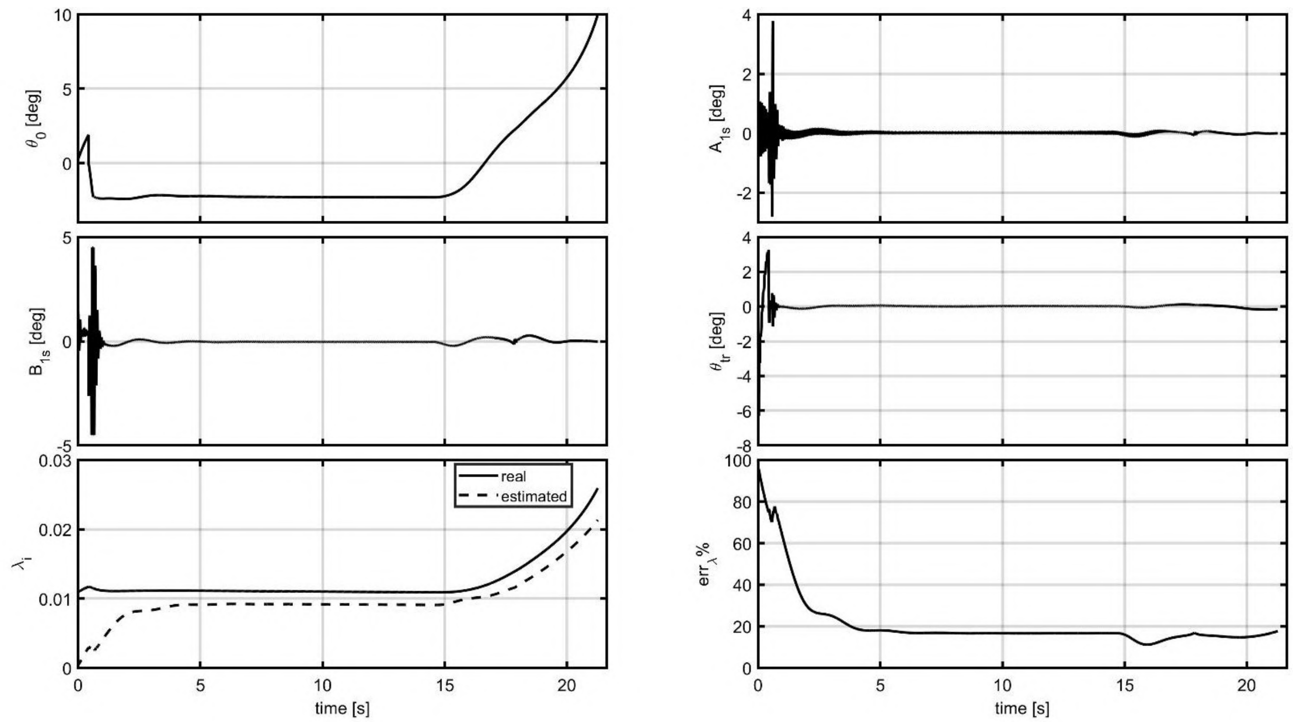

Figure 10: Commands and inflow estimation for the autorotation maneuver